Inorganic Chemistry

Article

A U(V) Chalcogenide: Synthesis, Structure, and Characterization of K$_2$Cu$_3$US$_5$

Danielle L. Gray,[†] Lisa A. Backus,[†] Hans-Albrecht Krug von Nidda,[‡] S. Skanthakumar,[§] Alois Loidl,[‡] L. Soderholm,[§] and James A. Ibers*,[†]

Department of Chemistry, Northwestern University, Evanston, Illinois 60208, Institut für Physik, Universität Augsburg, Augsburg, Germany, and Chemistry Division, Argonne National Laboratory, Argonne, Illinois 60439

The compound K$_2$Cu$_3$US$_5$ was obtained by the reaction of K$_2$S, UCl$_4$, CuCl, and S at 973 K. K$_2$Cu$_3$US$_5$ crystallizes in a new structure type in space group *Cmcm* of the orthorhombic system in a cell of dimensions $a = 3.9374(6)$ Å, $b = 13.813(2)$ Å, $c = 17.500(3)$ Å, and $V = 951.8(2)$ Å^3 at 153 K. The structure comprises $^{2}_{\infty}$[UCu$_3$S$_5$$^{2-}$] slabs separated by K$^+$ cations. The slabs are built from CuS$_4$ tetrahedra and US$_6$ octahedra. Their connectivity differs from other known octahedral/tetrahedral packing patterns. In the temperature range 130–300 K the compound exhibits Curie–Weiss magnetic behavior with $\mu_{eff} = 2.45(8)$ μ_B. This result together with both the bond distances and bond valence calculations and the absence of a Cu^{2+} ESR signal support the formulation of the above compound as K$^+$$_2Cu^+$$_3$U^{5+}S^{2-}$_5$.

Introduction

Although the chemistry of uranium is well documented,[1] the literature on U^{5+} remains meager compared to that on U^{3+}, U^{4+}, or U^{6+}. This is not surprising because of the tendency of U^{5+} in solution to disproportionate to U^{4+} and U^{6+} as well as the sensitivity of U^{5+} to oxidation. Compounds of U^{5+} mainly comprise the halides, alkoxides, oxides, and oxyhalides,[2] but a few other types of compounds are also known. A recent example[3] of a U^{5+} compound is the silicate K(UO)Si$_2$O$_6$, which contains a UO$_6$ octahedron made up from four equatorial silicate oxygen and two axial oxygen atoms. Another recent compound is K$_6$Cu$_{12}$U$_2$S$_{15}$.[4] There are no S−S bonds in this compound so that charge balance could have been achieved with Cu$^+$, U^{6+}, and S^{2-}. However, from conductivity measurements on pressed pellets and an analy-sis[5] of the magnetic measurements on ground single crystals the compound was given a nonclassical formulation, namely K$^+$$_6Cu^+$$_{12}$ U^{5+}$_2$S^{2-}$_{13}$S$^-$$_2$.

In addition to K$_6$Cu$_{12}$U$_2$S$_{15}$[4] in the A/Cu/U/Q system (A = alkali metal; Q = S, Se, or Te) the compounds CsCuUTe$_3$,[6] KCuUSe$_3$,[7] and CsCuUSe$_3$[8] are known. These three compounds of U^{4+} adopt the robust KCuZrS$_3$ structure type.[9] We report here the synthesis, structure, and characterization of the new A/Cu/U/Q compound K$_2$Cu$_3$US$_5$. We present evidence for a classical formulation of this compound as K$^+$$_2Cu^+$$_3$U^{5+}S^{2-}$_5$.

Experimental Section

Synthesis of K$_2$Cu$_3$US$_5$. CCl$_4$ was dried over KH and distilled. The following reagents were used as obtained from the manufac-turer: K (Cerac, 98%), S (Mallinckrodt, 99.6%), CuCl (Aldrich, 99+%), UO$_3$ (Kerr-McGee Nuclear Corp.), and hexachloropropene (Aldrich, 96%). K$_2$S was prepared by the stoichiometric reaction of the elements in liquid NH$_3$. UCl$_4$ was prepared by a modification

* To whom correspondence should be addressed. Phone: +1 847 491 5449. Fax: +1 847 491 2976. E-mail: ibers@chem.northwestern.edu.
† Northwestern University.
‡ Universität Augsburg.
§ Argonne National Laboratory.

 (1) Grenthe, I.; Drozdzynski, J.; Fujino, T.; Buck, E. C.; Albrecht-Schmitt, T. E.; Wolf, S. F. In *The Chemistry of the Actinide and Transactinide Elements*, Third ed.; Morss, L. R., Edelstein, N. M., Fuger, J., Eds.; Springer: Dordrecht, 2006; Vol. 1, pp 253−698.
 (2) Selbin, J.; Ortego, J. D. *Chem. Rev.* **1969**, *69*, 657−671.
 (3) Chen, C.-S.; Lee, S.-F.; Lii, K.-H. *J. Am. Chem. Soc.* **2005**, *127*, 12208−12209.
 (4) Sutorik, A. C.; Patschke, R.; Schindler, J.; Kannewurf, C. R.; Kanatzidis, M. G. *Chem.—Eur. J.* **2000**, *6*, 1601−1607.

 (5) Schilder, H.; Speldrich, M.; Lueken, H.; Sutorik, A. C.; Kanatzidis, M. G. *J. Alloys Compd.* **2004**, *374*, 249−252.
 (6) Cody, J. A.; Ibers, J. A. *Inorg. Chem.* **1995**, *34*, 3165−3172.
 (7) Sutorik, A. C.; Albritton-Thomas, J.; Hogan, T.; Kannewurf, C. R.; Kanatzidis, M. G. *Chem. Mater.* **1996**, *8*, 751−761.
 (8) Huang, F. Q.; Mitchell, K.; Ibers, J. A. *Inorg. Chem.* **2001**, *40*, 5123−5126.
 (9) Mansuetto, M. F.; Keane, P. M.; Ibers, J. A. *J. Solid State Chem.* **1992**, *101*, 257−264.

of the literature procedure.[10] A 3.00 g (10.5 mmol) portion of UO_3 was combined with 7.5 mL (53.2 mmol) of hexachloropropene in a 150 mL round-bottom flask. The flask was fit with a condenser and placed under an N_2 atmosphere that was vented through a KOH bubbler. The N_2 had been passed over BASF catalyst at 80 °C and then over Drierite to remove H_2O and O_2. The flask was gradually heated to 130 °C. This initiated an exothermic reaction that turned the solution into a deep-red color and released Cl_2 gas. Once the exothermic reaction was complete, the reaction mixture was allowed to reflux at 158 °C for 3.5 h. The resulting green UCl_4 was separated from the solution by filtration through a cannula. Three successive washes of the product with 10 mL portions of CCl_4 were carried out. Residual CCl_4 was removed under vacuum.

The initial reaction mixture consisted of 14.3 mg of CuCl (0.14 mmol), 25.1 mg of UCl_4 (0.066 mmol), and 21.5 mg of K_2S (0.19 mmol). Under an Ar atmosphere in a glovebox, the reaction mixture was loaded into a fused-silica tube that was evacuated to ∼10^4 Torr and flame sealed. The tube was placed in a computer-controlled furnace where it was heated to 623 K in 48 h, kept at 623 K for 48 h, heated again to 973 K in 72 h, and cooled at 14 K/h to 373 K, when it was removed from the furnace. The product was washed with deionized water to remove salt byproducts and was dried with acetone. The compound characterized as $K_2Cu_3US_5$ crystallizes as black needles and plates. Once the composition was established, a more rational synthesis was found. This proceeded from the reaction mixture of CuCl (0.42 mmol), UCl_4 (0.14 mmol), K_2S (0.60 mmol), and S (0.5 mmol). This mixture was subjected to the same heating cycle as that of the initial reaction mixture. $K_2Cu_3US_5$ was obtained in 24 wt % yield relative to U. It is air and moisture stable for several weeks. Semi-qualitative EDX analysis of selected crystals with a Hitachi S 3500 SEM showed an average ratio of K:Cu:U:S of 2:3:1:5. No Cl was detected.

Structure Determination. Single-crystal X-ray diffraction data were collected with the use of graphite-monochromatized Mo Kα radiation ($\lambda = 0.71073$ Å) at 153 K on a Bruker Smart 1000 CCD diffractometer.[11] The crystal-to-detector distance was 5.023 cm. Crystal decay was monitored by re-collecting 50 initial frames at the end of data collection. Data were collected by scan of 0.3° in ω in groups of 606, 606, 606, and 606 frames at φ settings of 0°, 90°, 180°, and 270°. The exposure time was 15 s/frame. The collection of intensity data was carried out with the program SMART.[11] Cell refinement and data reduction were carried out with the use of the program SAINT,[11] and face-indexed absorption corrections were performed numerically with the use of the program XPREP.[12] Then the program SADABS[11] was employed to make incident beam and decay corrections.

The structure was solved with the direct methods program SHELXS and refined with the full-matrix least-squares program SHELXL of the SHELXTL suite of programs.[12] The program STRUCTURE TIDY[13] was used to standardize the positional parameters. Additional experimental details are shown in Table 1 and in Supporting Information. Selected metrical data are presented in Table 2.

Electron Spin Resonance Measurements. Electron spin resonance (ESR) measurements in the temperature range 4.2−300 K

(10) Hermann, J. A.; Suttle, J. F. In *Inorganic Synthesis*; Moeller, T., Ed.; McGraw-Hill Book Company: New York, 1957; Vol. 5, pp 143−145.
(11) *SMART* Version 5.054 Data Collection *and SAINT-Plus* Version 6.45A Data Processing Software for the *SMART* System; Bruker Analytical X-Ray Instruments, Inc.: Madison, WI, U.S.A., 2003.
(12) Sheldrick, G. M. *SHELXTL* Version 6.14; Bruker Analytical X-Ray Instruments, Inc.: Madison, WI, U.S.A., 2003.
(13) Gelato, L. M.; Parthé, E. *J. Appl. Crystallogr.* **1987**, *20*, 139−143.
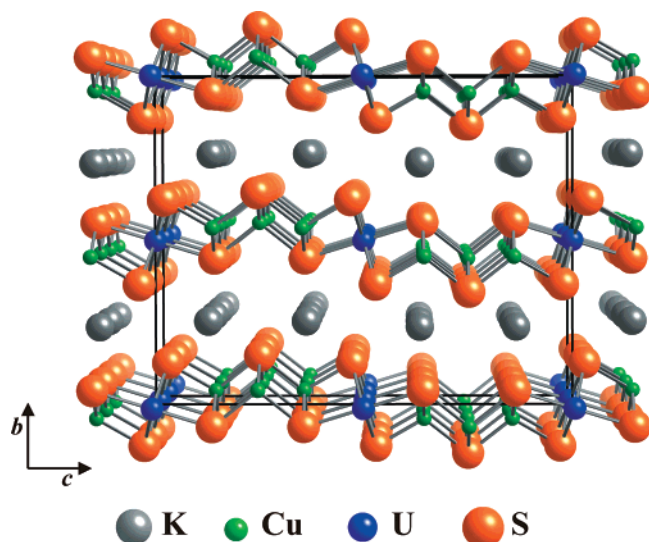
Table 1. Crystal Data and Structure Refinement for $K_2Cu_3US_5$

formula mass (amu)	667.15	T (K)	153(2)
space group	*Cmcm*	λ (Å)	0.71073
Z	4	ρ_c (g cm^{-3})	4.656
a (Å)	3.9374(6)	μ (cm^{-1})	254.68
b (Å)	13.813(2)	$R(F)^a$	0.0229
c (Å)	17.500(3)	$R_w(F^2)^b$	0.0554
V (Å^3)	951.8(2)		

$^a R(F) = \Sigma||F_o| - |F_c||/\Sigma|F_o|$ for $F_o^2 > 2\sigma(F_o^2)$. $^b R_w(F_o^2) = [\Sigma \, w(F_o^2 - F_c^2)^2/\Sigma wF_o^4]$, $w^{-1} = \sigma^2(F_o^2) + (0.02 \, F_o^2)^2$ for $F_o^2 \geq 0$; $w^{-1} = \sigma^2(F_o^2)$ for $F_o^2 < 0$.

Table 2. Selected Distances (Å) and Angles (deg) for $K_2Cu_3US_5$

Cu(1)−S(1)	2.356(1)	K(1)−S(1) × 2	3.236(1)
Cu(1)−S(2)	2.317(2)	K(1)−S(2)	3.240(2)
Cu(1)−S(3) × 2	2.3904(9)	K(1)−S(2) × 2	3.295(2)
Cu(2)−S(3) × 2	2.356(1)	K(1)−S(3) × 3	3.195(2)
Cu(2)−S(2) × 2	2.429(2)	Cu(1)−Cu(2)	2.7093(5)
U(1)−S(2) × 4	2.6827(9)	Cu(1)−U(1)	3.2543(6)
U(1)−S(3) × 2	2.587(1)		
S(3)−U(1)−S(3)	180	S(3)−Cu(1)−S(2)	105.34(4)
S(2)−U(1)−S(2)	94.42(4)	S(2)−Cu(1)−S(1)	112.22(6)
S(2)−U(1)−S(2)	85.58(4)	S(1)−Cu(2)−S(1)	113.34(9)
S(2)−U(1)−S(3)	89.49(4)	S(1)−Cu(2)−S(3)	110.02(3)
S(3)−Cu(1)−S(3)	110.89(6)	S(3)−Cu(2)−S(3)	102.94(8)
S(3)−Cu(1)−S(1)	111.38(4)		

were performed on two single crystals of $K_2Cu_3US_5$ with the use of a Bruker ELEXSYS E500 CW spectrometer equipped with a continuous He-gas-flow cryostat (Oxford Instruments). Measurements were made at both X-band (9.47 GHz) and Q-band (34 GHz) frequencies. The ESR measurement detects the power P absorbed by the sample from the transverse magnetic microwave field as a function of the static magnetic field H. Fields up to 18 kOe were used. The signal-to-noise ratio of the spectra was improved by recording the derivative dP/dH with the use of a lock-in technique with field modulation. The sensitivity of the spectrometer is about $10^{11}−10^{13}$ spins/Oe line width.

Magnetic Susceptibility Measurements. The magnetic susceptibility data were collected on a Quantum Design MPMS XL7 SQUID magnetometer from a 5 mg sample of ground single crystals of $K_2Cu_3US_5$ that had been loaded into a gelatin capsule. Variable-temperature experiments were carried out between 5 and 320 K with applied fields of 0.1, 1, 2, 5, and 10 kOe. Field measurements, to a maximum of 30 kOe, were carried out at several temperatures.

Results

Synthesis. The synthesis of $K_2Cu_3US_5$ proceeded from a partial metathesis reaction of K_2S, CuCl, UCl_4, and S at a reaction temperature of 973 K. Small black crystals of high quality were obtained in approximately 24 wt % yield. $K_2Cu_3US_5$ is moderately stable in air.

Structure. $K_2Cu_3US_5$ crystallizes in a new structure type (Figure 1). The structure consists of $_\infty^2[UCu_3S_5^{2-}]$ slabs separated by K^+ centers. Each U atom, which is located at a site of symmetry 2/*m*., is octahedrally coordinated by six S atoms. There are two crystallographically independent Cu atoms in the asymmetric unit. The Cu(1) atom has site symmetry *m*.. whereas the Cu(2) atom has site symmetry *mm*... In the structure each is tetrahedrally coordinated by four S atoms. Figure 2 shows a $_\infty^2[UCu_3S_5^{2-}]$ layer. Within each layer, US_6 octahedra edge share and CuS_4 tetrahedra corner share with like polyhedra along the [100] direction to form chains. The US_6 octahedra edge share with four Cu-
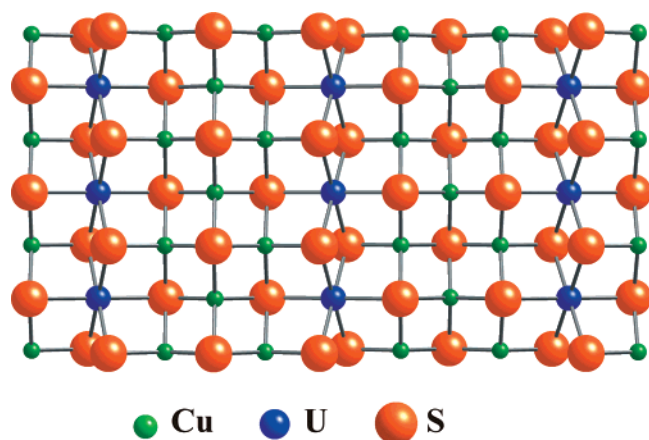
Figure 1. Structure of $K_2Cu_3US_5$ as viewed down [100].

Figure 2. $^2_\infty[UCu_3S_5{}^{2-}]$ layer as viewed down [010].

(1)S_4 tetrahedra, thereby connecting the U chains to Cu(1) chains on both sides in the [001] direction. Each Cu(1)S_4 tetrahedron edge shares with two US_6 octahedra on one side and two Cu(2)S_4 tetrahedra on the other. The chains pack along [001] in a U(1)*oct*, Cu(1)*tet*, Cu(2)*tet*, Cu(1)*tet*, U(1)-*oct* pattern to form the $^2_\infty[UCu_3S_5{}^{2-}]$ layer. This connectivity within the $^2_\infty[UCu_3S_5{}^{2-}]$ layer is different from other known octahedral/tetrahedral packing patterns. In NaCuTiS$_3$[14] the connectivity within the layer is *oct oct tet tet oct oct*, in NaCuZrS$_3$[14] it is *oct tet oct tet oct tet*, in Na$_2$Cu$_2$ZrS$_4$[15] it is *oct tet tet oct tet tet*, and in K$_3$Cu$_3$Th$_2$S$_7$[16] the connectivity within the layer is *oct tet oct tet tet*.

Each K center, located at a site with symmetry $m..$, is coordinated by a capped trigonal prism of seven S atoms. Each capped trigonal prism has two face-sharing neighbors along [100] and three edge-sharing ones along [001] to form a $^2_\infty[K_2S_5{}^{8-}]$ layer, as shown in Figure 3.

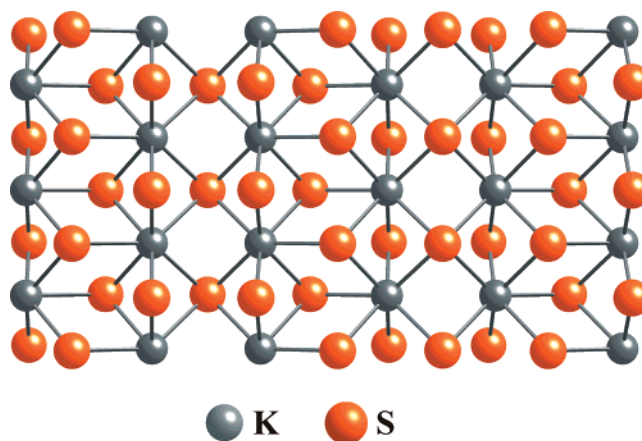**Figure 3.** $^2_\infty[K_2S_5{}^{8-}]$ layer as viewed down [010].

Electron Spin Resonance. Two single crystals of $K_2Cu_3US_5$ (with an estimated spin concentration of about 10^{15} Cu spins, if Cu^{2+} were present in the compound) have been measured between 4.2 and 300 K at 9.47 and 34 GHz. No signal was detectable, and there was no indication of even a slight deviation from background. Neither a Cu^{2+} nor a U signal was visible.

The absence of a U signal is not surprising. Uranium signals can be too broad to detect because of strong spin−orbit coupling and fast spin fluctuations. This phenomenon is also seen in some Ce compounds such as CeNiSn.[17] Because of strong relaxation, a Cu^{2+} signal can be too broad to detect as is the case in the high-temperature supercon-ducting cuprates.[18] On the other hand, in one-dimensional spin $^1/_2$ systems with Cu^{2+} or V^{4+} the signal is often detected and can be narrow as, for example, in CuGeO$_3$.[19] In principle, if the Cu^{2+}:Cu$^+$ ratio in $K_2Cu_3US_5$ were 1:2, the situation would be similar to that in Na$_{1/3}$V$_2$O$_5$[20] where the V^{4+}:V^{5+} ratio is 1:5. In Na$_{1/3}$V$_2$O$_5$ the electrons are localized at low temperatures and a narrow ESR signal was detected. The signal broadened with increasing temperature.

Magnetic Susceptibility Measurements. The magnetic susceptibility of $K_2Cu_3US_5$ obtained as a function of tem-perature under a small applied field is shown in Figure 4. For the purpose of interpretation, the data are considered within two different temperature regimes: above 130 K where the behavior can be described in terms of noninter-acting spins, and below 108 K where there is evidence of magnetic correlations. Considering first the higher-temper-ature regime, we depict in Figure 5 the field dependence of the magnetic response obtained at 300 K. When one is interpreting susceptibility data, the magnetic response is normally assumed to be linear over the field range used to determine the magnetization; it is the slope of the *M* versus *H* curve that is the magnetic susceptibility at the temperature

(14) Mansuetto, M. F.; Keane, P. M.; Ibers, J. A. *J. Solid State Chem.* **1993**, *105*, 580−587.
(15) Mansuetto, M. F.; Ibers, J. A. *J. Solid State Chem.* **1995**, *117*, 30−33.
(16) Llanos, J.; Cortés, R.; Guizouarn, T.; Peña, O. *Mater. Res. Bull.* **2006**, *41*, 1266−1271.

(17) Mair, S.; Krug von Nidda, H.-A.; Lohmann, M.; Loidl, A. *Phys. Rev. B* **1999**, *60*, 16409−16414.
(18) Elschner, B.; Loidl, A. In *Handbook on the Physics and Chemistry of the Rare Earths*; Gschneidner, K. A., Jr., Eyring, L., Maple, M. B., Eds.; Elsevier: Amsterdam, 2000; Vol. 30, pp 375−415.
(19) Eremina, R. M.; Eremin, M. V.; Glazkov, V. N.; Krug Von Nidda, H.-A.; Loidl, A. *Phys. Rev. B* **2003**, *68*, 014417-1−014417-10.
(20) Riedel, E.; Karl, R.; Rackwitz, R. *Mater. Res. Bull.* **1977**, *12*, 599−603.
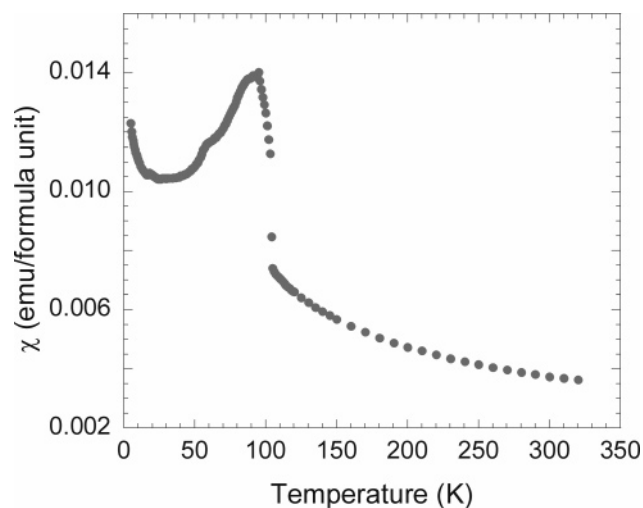
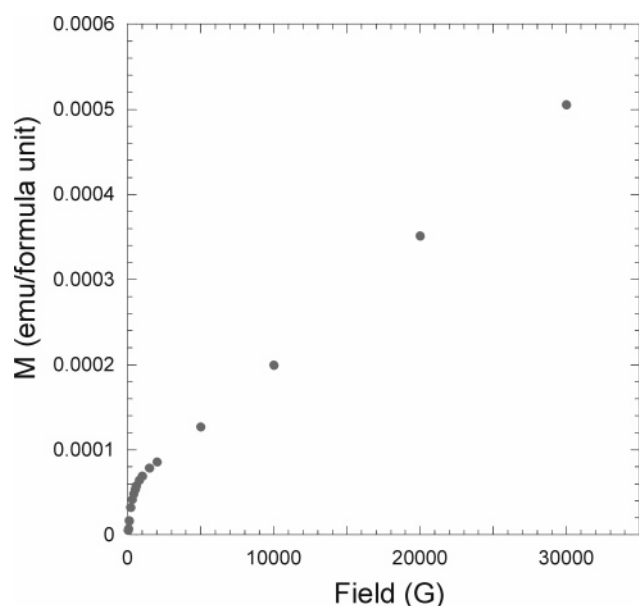**Figure 4.** Magnetic susceptibility of $K_2Cu_3US_5$ obtained as a function of temperature under an applied field of 100 Oe.

Figure 5. Magnetization per formula unit of $K_2Cu_3US_5$ plotted as a function of field measured at 300 K.

of the measurement. It can be seen from Figure 5 that the response is nonlinear at fields lower than 1000 G. Above this applied field, this contribution to the measured magnetization becomes field independent and an additive constant to the total magnetization. This field-independent term, 5.38×10^{-5} emu at 300 K, represents about 10% of the measured response from our 5 mg sample at a field of 30 kOe.

The field-independent term may be removed from the measurements by obtaining M versus T data under several different applied fields (1, 2, 5, and 10 kOe) and subtracting data from two different fields. Comparing difference data from the combination of different applied fields revealed that this procedure produced susceptibility versus temperature data that agreed within 2% accuracy for applied fields >2 kOe. The origin of the field-independent magnetization is unknown, but such behavior is often interpreted in terms of a saturated ferromagnetic component. In the present instance, the field-independent magnetization is consistent with a ferromagnetic contribution with ordering temperature much
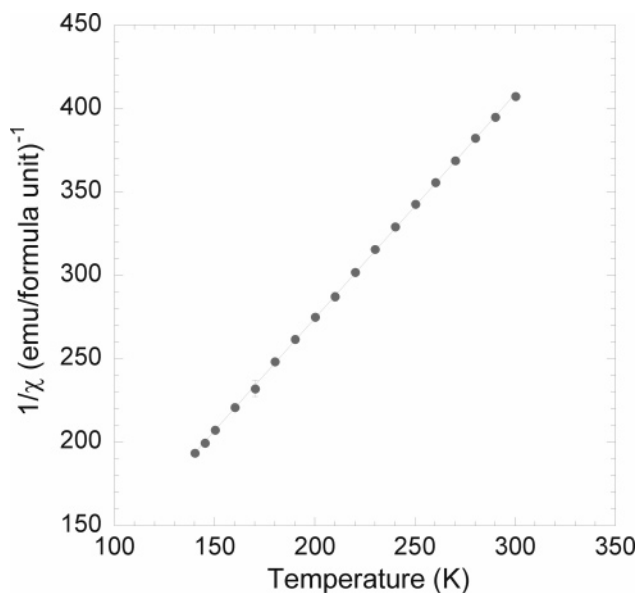

Figure 6. Inverse susceptibility per formula unit of $K_2Cu_3US_5$ plotted as a function of temperature. This plot was obtained by subtracting from each magnetization point obtained under an applied field of 5000 Oe the corresponding point obtained under an applied field of 2000 Oe. The fit to the Curie−Weiss equation is shown as a solid line.

higher than the temperature range of the experiment. A possible source of such a ferromagnetic contribution is metallic Fe. A total of about 0.005 wt %, that is 0.25 μg of Fe in the 5 mg sample, would account for the observation. That amount would go undetected analytically.

A representative plot of inverse magnetic susceptibility versus temperature obtained in this manner is shown in Figure 6. The data are linear over the temperature range of 130−300 K, indicating classical Curie−Weiss behavior, $\chi = C/(T - \Theta)$, in which C is the Curie constant, related to the effective moment by $\mu_{eff} = (8C)^{1/2}$, and Θ is the Weiss constant, a term meant to account for moment correlations or the influence of low-lying crystal-field states. From a least-squares fit to these data we find an effective moment μ_{eff} of 2.45(8) μ_B and a Weiss constant of 4(1) K.

The magnetic response shows deviations from the behavior expected for a classic paramagnet at temperatures below 108 K. A sharp increase in the susceptibility is observed over the temperature range 94−105 K with a minimum in the first derivative at 104(2) K. There is a sudden change of slope at 94(2) K with a decreasing susceptibility observed between about 94 and 20 K. At even lower temperatures, there is an upturn in the measured signal with decreasing temperature. Despite the general cusp in the susceptibility over the temperature range of about 50−104 K, the overall complex response is not indicative of a simple antiferromagnetic ordering. Instead, the low-temperature response appears to have a complex origin, which could involve a magnetic or a structural phase change, the latter of which could be coupled with Cu−U charge transfer.

Discussion

There are no S−S bonds in the structure of $K_2Cu_3US_5$, the shortest S···S interaction being 3.645 Å. Therefore, the

formal oxidation state of S in $K_2Cu_3US_5$ may be assigned as -2. Thus, the combined formal oxidation states of three Cu atoms and one U atom must be $+8$ to achieve charge balance. This can be accomplished with three Cu^+ and one U^{5+} or two Cu^+, one Cu^{2+}, and one U^{4+}. The Cu^{2+} oxidation state is rarely, if ever, found in sulfides, which makes it likely that $K_2Cu_3US_5$ is a compound of U^{5+}. The absence of a Cu^{2+} ESR signal also suggests U^{5+}. Further, indirect evidence for this comes from the bond distances. Although the Cu−S distances, ranging from 2.317(2) to 2.429(2) Å, are normal (e.g., 2.319(1)−2.540(2) Å in $RbEr_2Cu_3S_5$[21] and 2.305(1)−2.381(1) Å in $Ba_2Cu_2US_5$[22]), the U−S distances of 2.587(1) and 2.6827(9) Å are shorter than those in most US_6 octahedra that involve U^{4+}, for example, 2.680(5)−2.709(5) Å in $BaUS_3$[23,24] and 2.673(2)−2.770(1) Å in $Ba_2Cu_2US_5$.[22]

Bond valence sums[25] of U = 4.732, Cu(1) = 1.029, and Cu(2) = 0.952 also suggest the presence of U^{5+}.

Finally, the value of μ_{eff} of 2.45(8) μ_B may be compared to the corresponding values of the two proposed models for formal oxidation states within the compound $K_2Cu_3US_5$: (i) three Cu^+ and one U^{5+}, or (ii) one Cu^{2+}, two Cu^+, and one U^{4+}. Cu^+ has no temperature dependence to its susceptibility whereas Cu^{2+} has one unpaired d spin and a spin-only effective moment of 1.73 μ_B. U^{5+}, an ^1f spin system modeled within the Russell−Saunders coupling formalism,[26] has a free-ion effective moment of 2.54 μ_B whereas U^{4+} with two unpaired f spins and a $^3H_4$ ground term has a free-ion effective moment of 3.58 μ_B.[27] Assuming these values, we find that the formal oxidation-state model (i), involving U^{5+}, has a free-ion calculated moment of 2.54 μ_B whereas the model (ii), which includes U^{4+} and Cu^{2+}, has a calculated moment of 3.98 μ_B. The close correspondence of the measured moment of 2.45(8) μ_B to that of 2.54 μ_B for model (i) is corroborative evidence for the presence of U^{5+} in the sample.

In summary, the structural evidence, the valence bond calculation, the absence of a Cu^{2+} ESR signal, and the μ_{eff} value are all consistent with $K_2Cu_3US_5$ being a classical compound containing the rare oxidation state U^{5+}.

Supporting Information Available: The crystallographic file in CIF format for $K_2Cu_3US_5$. This information is available free of charge via the Internet at http://pubs.acs.org.

IC700774G

(21) Huang, F. Q.; Ibers, J. A. *J. Solid State Chem.* **2001**, *158*, 299−306.
(22) Zeng, H.-Y.; Yao, J.; Ibers, J. A. Unpublished work.
(23) Lelieveld, R.; IJdo, D. J. W. *Acta Crystallogr., Sect. B: Struct. Crystallogr. Cryst. Chem.* **1980**, *36*, 2223−2226.
(24) Brochu, R.; Padiou, J.; Grandjean, D. *C. R. Seances Acad. Sci., Ser. C* **1970**, *271*, 642−643.
(25) O'Keeffe, M. *Acta Crystallogr., Sect. A: Cryst. Phys., Diffr., Theor. Gen. Crystallogr.* **1990**, *46*, 138−142.
(26) Staub, U.; Soderholm, L. In *Handbook on the Physics and Chemistry of Rare Earths*; Gschneidner, K. A., Jr., Eyring, L., Maple, M. B., Eds.; Elsevier: Amsterdam, 2000; Vol. 30, pp 491−545.
(27) Pitzer, K. S. *Quantum Chemistry*; Prentice Hall: New York, 1953; p 529.